Iranian Journal of Basic Medical Sciences

ijbms.mums.ac.ir

IJBMS

Investigation on metabolism of cisplatin resistant ovarian cancer using a genome scale metabolic model and microarray data

Ehsan Motamedian [1, 2], Ghazaleh Ghavami [2, 3], Soroush Sardari [2 *]

[1] Biotechnology Group, Department of Chemical Engineering, Tarbiat Modares University, Tehran, Iran
[2] Drug Design and Bioinformatics Group, Medical Biotechnology Department, Biotechnology Research Center, Pasteur Institute of Iran, Tehran, Iran
[3] Eastern Mediterranean Health Genomics and Biotechnology Network (EMGEN), Tehran, Iran

ARTICLE INFO

Article type:
Original article

Article history:
Received: Apr 20, 2014
Accepted: Feb 18, 2015

Keywords:
Cisplatin resistance
Drug target
Lactate
Metabolism
Microarray
Warburg effect

ABSTRACT

Objective(s): Many cancer cells show significant resistance to drugs that kill drug sensitive cancer cells and non-tumor cells and such resistance might be a consequence of the difference in metabolism. Therefore, studying the metabolism of drug resistant cancer cells and comparison with drug sensitive and normal cell lines is the objective of this research.
Material and Methods: Metabolism of cisplatin resistant and sensitive A2780 epithelial ovarian cancer cells and normal ovarian epithelium has been studied using a generic human genome-scale metabolic model and transcription data.
Result: The results demonstrate that the most different metabolisms belong to resistant and normal models, and the different reactions are involved in various metabolic pathways. However, large portion of distinct reactions are related to extracellular transport for three cell lines. Capability of metabolic models to secrete lactate was investigated to find the origin of Warburg effect. Computational results introduced SLC25A10 gene, which encodes mitochondrial dicarboxylate transporter involved in exchanging of small metabolites across the mitochondrial membrane that may play key role in high growing capacity of sensitive and resistant cancer cells. The metabolic models were also used to find single and combinatorial targets that reduce the cancer cells growth. Effect of proposed target genes on growth and oxidative phosphorylation of normal cells were determined to estimate drug side-effects.
Conclusion: The deletion results showed that although the cisplatin did not cause resistant cancer cells death, but it shifts the cancer cells to a more vulnerable metabolism.

► *Please cite this paper as:*
Motamedian E, Ghavami Gh, Sardari S. Investigation on metabolism of cisplatin resistant ovarian cancer using a genome scale metabolic model and microarray data. Iran J Basic Med Sci 2015; 18: 267-276.

Introduction

Cisplatin is the first-line therapy for the treatment of ovarian cancer as the most deadly gynecological disease, but resistance to this drug occurs in many cases (1). While most patients initially treated with surgical debulking and chemotherapy based on platinum-based drugs (2), relapse of disease with fully chemoresistance is observed for over 80 percent of treated patients (3). The cause and mechanism of chemoresistance is not well known (4).

Studying the metabolism of cisplatin resistant and sensitive cancer cells may lead to find the causes of chemoresistance. Furthermore, metabolism has a key role in many epidemic human diseases especially cancer, and hence targeting cancer metabolism has emerged as a motivating topic for drug discovery (5, 6). In recent years, cancer therapy with targeting metabolic pathways has been taken into consideration by researchers (7). Targeting cancer metabolism requires information about human metabolic network and how different cancers use this metabolic network in comparison with normal cells (7). Only a thorough understanding will lead to find the targets that can be of therapeutic benefit with minimum side-effect on normal cells.

Metabolic network reconstruction has become a common tool for studying the metabolism of the cells (8). In the recent years, various human metabolic networks have been reconstructed. The first genome-scale reconstruction of the global (non-

*Corresponding author: Soroush Sardari. Drug Design and Bioinformatics Group, Medical Biotechnology Department, Biotechnology Research Center, Pasteur Institute of Iran, #69, Pasteur Avenue, Tehran, Iran and Eastern Mediterranean Health Genomics and Biotechnology Network (EMGEN), #69, Pasteur Avenue, Tehran 13164, Iran; Tel/Fax: +98-21-66954324; email: sardari@pasteur.ac.ir

tissue specific) human metabolic network, named Recon 1 (9) was reconstructed based on an extensive evaluation of genomic and bibliomic data. Recon 1 was updated to the last global human metabolic reconstruction named Recon 2. The model expansion was carried out at reconstruction 'jamboree' meetings (10) that domain experts share their knowledge to consider biochemical knowledge from existing reconstructions and published literature.

Many studies have shown similar metabolic states occurring across tumor cells (11-13). For example, many types of cancer cells adapt their metabolism to facilitate biomass formation to enable proliferation (11). According to this characteristic of cancer cells, flux balance analysis (FBA) that is a constraint-based modeling approach could be applicable to predict alterations in cancer metabolism using genome-scale metabolic models. This approach has been successfully used in the past to simulate the growth of fast growing microorganisms (14, 15). FBA commonly considers growth rate as objective function and it searches for metabolic flux distributions that produce essential biomass precursors at high rates, and hence this approach is appropriate for modeling cancer metabolism (14). Warburg effect (a phenomenon revealed by Otto Warburg in 1924) is an important characteristic of cancer cells that results in changes in glucose metabolism and an increase in biosynthetic activities such as nucleotide, lipids and amino-acid synthesis and is important for cellular proliferation (7, 16). This effect indicates an increase in the inefficient production of ATP via glycolysis resulting in the secretion of non-oxidized carbons in the form of lactate, even in the presence of oxygen (named aerobic glycolysis) (17). Aerobic glycolysis produces only 2 ATP molecules per one glucose molecule, whereas oxidative phosphorylation results in the generation of 32 ATP molecules per one molecule of glucose (17).

The global models have been used for the automated reconstruction of cell-specific and tissue-specific models using various high throughput data (18). Because of the abundance of transcriptomic data, several FBA-driven algorithms have been proposed that incorporate gene expression profiles into metabolic flux constraints such as GIMME (19), E-flux (20), iMAT (21) Moxely (22), MADE (23), RELATCH (24), INIT (25) and mCADRE (26) and improve model predictions by deleting reactions or by constraining their activity levels. Each of these methods has advantages and disadvantages (18), and are selected based on the purpose of modeling.

According to the key role of metabolism in many major human diseases especially cancer, metabolic reconstructions have been applied to guide experiments. Folger *et al* (11) built a core metabolic model of cancer metabolism for the NCI-60 cancer cell lines to propose drug targets. Li *et al* (27) presented a computational method to predict new targets for approved anti-cancer drugs using Recon 1. Jerby *et al* (28) developed the metabolic phenotypic analysis (MPA) method to conduct the first genome-scale study of breast cancer metabolism and predict the growth rates of cell lines, amino acid biomarkers and tumor lipid levels. Despite several studies conducted on cancer, metabolic models have not been used to predict the metabolic state of drug-resistant cancers.

In this paper, GIMME algorithm (29) was used to study metabolism of drug-resistant cancer in comparison with drug-sensitive cancerous and normal cell lines. With considering the proliferative cancer cells, the advantage of the GIMME is that it guarantees achieving to the cell growth as objective function based on gene expression levels. Considering a user-specified threshold and removing inactive reactions from the model is the main disadvantage of this algorithm. To eliminate the need for a user-specified threshold, a criterion based on absent/present predictions of MAS5 algorithm was used (30).

Recon 2 includes more orphan reactions identified using biochemical data for various human tissues in comparison with Recon 1. Among 7440 reactions of Recon 2, microarray data of HG-U133 Plus 2.0 Array used in this research could determine presence of 4194, while presence of 2245 of 3743 reactions in Recon 1 is determined using these transcription data. Therefore, it seems that using only microarray data is not adequate to reconstruct tissue-specific metabolic models using Recon 2. Hence, Recon 1 was used to reconstruct cell-specific models.

In this research, the metabolic models firstly used to find the differences in metabolic pathways utilization. After comparison of metabolisms, the ability of the cancer cells to secrete lactate in comparison with the normal cell was studied and the origins of different capabilities of metabolisms were searched. Furthermore, single gene deletion analysis to find metabolic target genes with minimum side-effect on normal cells and double gene deletion analysis to study the synergism of genes and to find metabolic target genes for combinatorial therapies were carried out.

Model and computational methods

Genome-scale model

Recon 1 (9) including 3742 reactions, 1905 genes and 2766 metabolites was used to construct a stoichiometric model. The model was integrated with gene expression data using GIMME (Gene Inactivity Moderated by Metabolism and Expression) algorithm (19) to construct cisplatin resistant and sensitive A2780 epithelial ovarian cancer models,

Table 1. Number of different reactions in the three metabolic models. For example, 42 reactions exist in the resistant model that are absent from sensitive model

	Not in the model		
In the model	Resistant	Sensitive	Normal
resistant	-	42	202
sensitive	38	-	179
normal	157	134	-

and also normal ovarian surface epithelium model. The GIMME algorithm first uses FBA to find the maximum possible flux through the required functionality (for example growth). Subsequently, GIMME compares the experimental mRNA levels to a user-specified threshold and removes reactions with mRNA levels below the given threshold from the model. However, if the reduced model is unable to achieve the required functionality, GIMME solves a linear programming problem that adds sets of the removed reactions back into the model, so that minimizes deviation from the expression data.

Used biomass formula of Shlomi *et al* (16) was added to the model and used as objective function to calculate growth rate. Details of the objective function are presented in the supplementary file 1 (Table S1). This objective function is appropriate for proliferative cancer cells. However, objective function of normal ovarian cells is not the maximization of growth rate and unlike cancer cells; they do not have rapid proliferation. However, growth rate was considered to compare growth ability of its network with two cancerous metabolic networks. For cancer models, microarray data of Li *et al* (1) (GSE15709), which performed five replicates for resistant and sensitive cells have been used. Construction of normal ovarian surface epithelium model was carried out based on the microarray data of Stany *et al* (31) (GSE29450) with ten replications.

Instead of using a user-defined threshold, active and inactive reactions were determined using detection call generated by MAS5 algorithm (30). Present, marginal and absent genes in each replicate were identified using an MAS5 algorithm (scores were given as present=2, marginal=1 and absent=0). If a gene was detected to be present in all replicates of cancer (normal) cells, sum of the values in 5 (10) replicates will be 10 (20). Therefore, we determined presentation of a gene in the cell based on the following rules.

1- If sum of the values in 5 (10) replicates was more than or equal to 7 (14), the corresponding gene is present.

2- If sum of the values in 5 (10) replicates was less than 7 (14) and more than or equal to 4 (8), the corresponding gene is marginal.

3- If sum of the values in 5 (10) replicates was less than 4 (8), the corresponding gene is absent.

Automatic reconstructed models include all present and marginal genes and minimum number of absent genes that are required for growth. Reduced models including 3279, 3278 and 3241 reactions and 2638, 2639 and 2649 metabolites for resistant, sensitive and normal cells were specified. All metabolic models are presented in supplementary file 2.

Simulation conditions and in silico experiments

RPMI-1640 medium was considered in all simulations (11), and the COBRA toolbox and GLPK package (32) was used for solving the model in the MATLAB software. Metabolites and maximum uptake of the growth medium are presented in the supplementary file 1 (Table S2). The medium values were applied in the model by limiting the lower bound of exchange reactions. To study on Warburg phenomenon, effect of lactate secretion rate on growth was determined. Also, growth rate was fixed at optimal value and maximum oxygen uptake rate and ATP synthase activity (for energy production using oxidative phosphorylation) were calculated by changing the objective function.

Six sets of *in silico* experiments were carried out to investigate the effect of single and double gene deletions on cells growth using FBA approach. A gene deletion in the model results in removal of the associated reactions. In single gene deletion, relative growth rate (GR) (growth rate predicted after gene knockout per growth rate predicted for wild type) was calculated for each gene, and lethal (GR=0), sick (growth reducing) (GR<1), and ineffective (GR=1) genes were determined. In double gene deletion, interactions between genes have been studied. Two genes have interactions if the calculated growth rate of strain with double deletion results in less growth rate than growth rate of either of single deletion strains. Two genes are synthetic lethal while their double deletion causes to GR equals to zero. In addition, two genes are named synthetic sick if their double deletion causes to GR less than one. In double deletion analysis, number of genes that interact with each gene has also been determined.

Results

Comparison of the metabolisms

Table 1 indicates the number of reactions present in each metabolic model in comparison with the other model. Furthermore, supplementary File 3 represents metabolism comparison of three cells. Maximum difference of the metabolisms belongs to resistant and normal models and they are distinct in 359 reactions, while number of different reactions for normal and sensitive models is 313. Sensitive and resistant cancer models with 80 distinct reactions are the most similar metabolic models as could be predicted. In fact, comparison of the models shows that resistance to cisplatin caused adding 42 reactions to the metabolism and removing 38 reactions from the metabolism.

Difference in metabolism activation of cells has been studied by comparing difference in used reactions and their metabolic pathways. Figures 1 (a) and (b) indicate distribution of different reactions for resistant and sensitive cancers in the metabolic pathways. The most differences belong to the exchange of the metabolites with extracellular environment, and extracellular exchange is more limited in resistant model. Genes belonging to 8 and 12 transport reactions were activated and inactivated, respectively in resistant model. The eight added reactions transport alanine, asparagine, glutamine and serine based on sodium-proton coupled system (associated gene: SLC38A5 or SLC38A3), biotin, pantothenate and lipoate via sodium symport channel (associated gene: SLC5A6) and urea and water co-transport (associated gene: SLC5A1). Removed exchange reactions include bicarbonate transport (Na/HCO3 1:2 and 1:3 co-transport), 5-hydroxy-L-tryptophan, adrenaline, dopamine, histamine and noradrenaline secretion via secretory vesicle (ATP driven), dopamine and histamine uniport and chloride (which there is in cisplatin structure) uptake via formate and iodide counter-transport. Amino acids metabolism especially tyrosine metabolism is the other importantly different metabolism in cancers. In central metabolism, glucose 6-phosphate dehydrogenase is active in normal and resistant models while it is inactivated in sensitive model.

Figures 1 (c) and (e) compare pathway usage of the resistant and normal models. The most important difference of these metabolic models belongs to transportation of metabolites similar to difference of resistant and sensitive models, but in addition to extracellular transport, they are distinct in lysosomal and mitochondrial transport. Genes belonging to 8 lysosomal and 21 mitochondrial transport reactions are active in resistant compared with normal metabolic model. Furthermore, this discrepancy could be observed by comparison of sensitive and normal models presented in Figures 1 (d) and (f). Hence, capability of metabolites transportation between cytoplasm and three extracellular medium, lysosome and mitochondria in cancer cells is developed. All eight lysosomal transport reactions were activated due to the SLC29A3 gene (ID: 55315) over expression. Deletion of this gene does not affect on cancer models growth. Five genes SLC29A1 (ID: 2030), SLC25A2 (ID: 83884), SLC25A15 (ID: 10166), SLC25A10 (ID: 1468) and ATP10A (ID: 57194) are responsible for different mitochondrial transport of cancerous cells. Genes SLC25A10 and SLC29A1 have the most contributions of 9 and 6 reactions, respectively, among 21 reactions.

Sector of other metabolisms in Figure 1 indicates the reactions belong to the other pathways. Generally, the Figure demonstrates that cancer cells usage of metabolism is very different from normal cells, and reactions from various pathways are activated or deactivated. This difference for resistant and sensitive cells is commonly identical. For example, three reactions in Glycolysis/Gluconeogenesis including fructose-bisphosphatase, phosphoenolpyruvate carboxykinase and acetyl-CoA synthetase have been omitted in both cancer cells. In some pathways, deviation of resistant metabolism from the normal metabolism is more evident. For instance, nucleotides pathway is more different in resistant and normal cells, and it may be due to the cisplatin effect on chromosome.

Metabolic origin of Warburg effect

The Warburg effect is one of the known phenotype in most of the cancer cells, and hence the metabolic models used to find the origin of this discrepancy in metabolism. As mentioned, cancer cells try to have maximum proliferation; hence, lactate secretion should not be in contrast to the high growth. To study this hypothesis, the models were forced to secrete lactate and its effect on growth was analyzed. Calculations presented in Figure 2 clearly indicate the robustness of cancer models' growth to lactate secretion compared with normal model. For cancer models, there is a range of lactate secretion rates between 0 and 6 mmol/gDWh in which their growth will be optimal. However, maximum growth occurs in zero lactate secretion rate for normal model that is equal to optimal growth of sensitive model, and increment of secretion sharply decreases the growth.

It can be seen in Figure 3 that cancer cells consume more oxygen at zero lactate production. Increase of lactate excretion results in reduction of oxygen demand especially for cancer cells. In fact, cancer cells select metabolisms that are able to reduce oxygen demand by more production of lactate, while growth is not affected. Oxygen demand with more lactate secretion in normal cells decreases along with lower intensity of cancer cells.

Figure 4 indicates that lactate secretion causes lower activity of ATP synthase. Indeed, tumors could produce ATP via oxygen-independent process of oxidative phosphorylation due to the lactate secretion. This phenotype is not observed for normal cells.

It is interesting that phenotype of cancer cells for lactate secretion is similar although their metabolisms are different. Therefore, there are some identical genes in both cancer cells in which they are responsible for this phenotype of cancer cells. These genes are absent from the normal model, and it is valuable to find them.

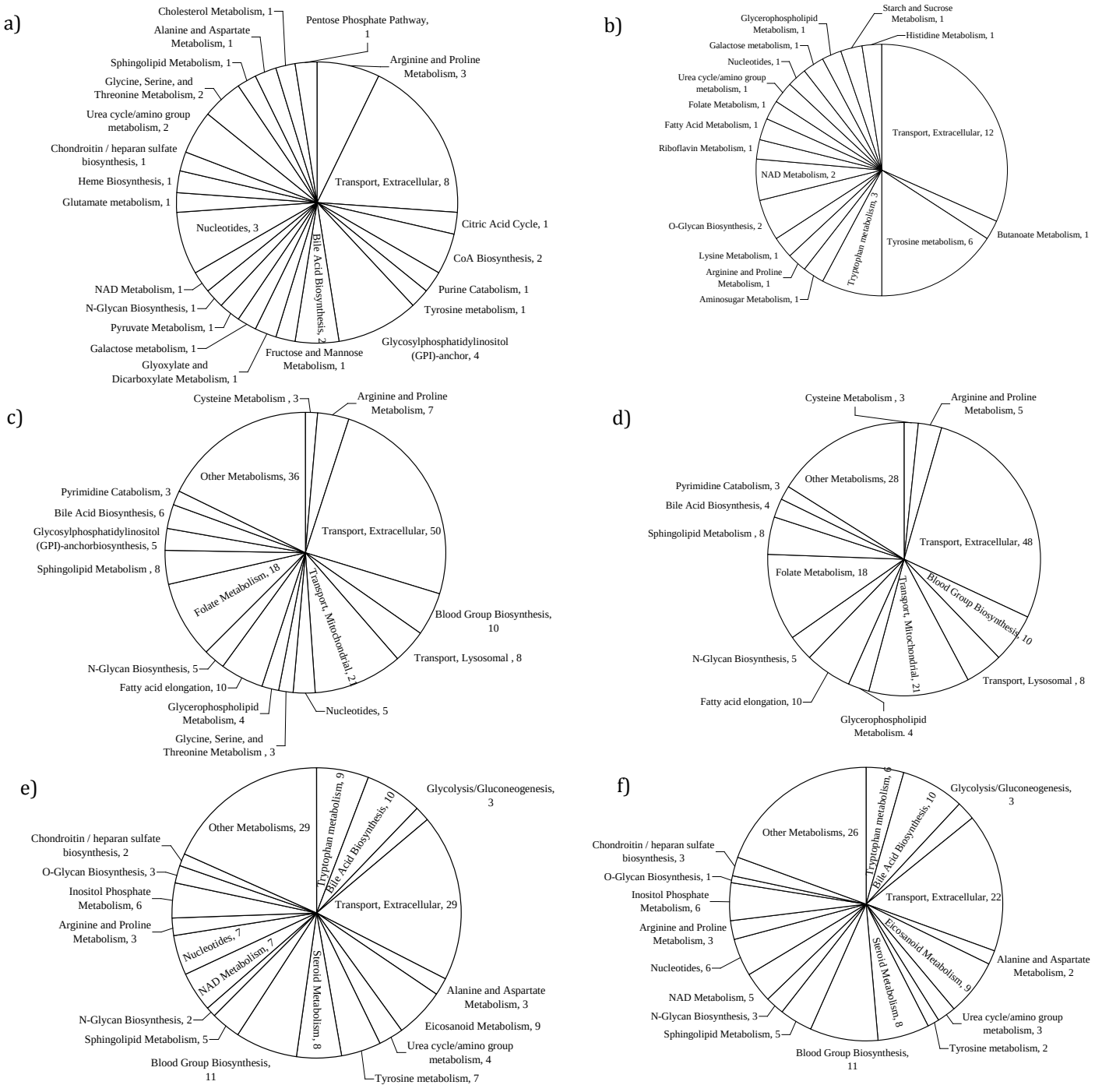

Figure 1. Number of reactions in each pathways which are present a) in resistant model and absent from sensitive model, b) in sensitive model and absent from resistant model, c) in resistant model and absent from normal model, d) in sensitive model and absent from normal model, e) in normal model and absent from resistant model, b) in normal model and absent from sensitive model

For this purpose, omitted genes from normal model were found. Among them, the genes that are expressed in sensitive and resistant models and their associated reactions were determined. There are 165 reactions that are expressed in the resistant and sensitive models, while they are not expressed in the normal model. These reactions were deleted from cancer models, and ability of the models to secrete lactate was investigated. There were eight groups of seven reactions that their deletion resulted in the lack of robustness of cancer models' growth to lactate secretion.

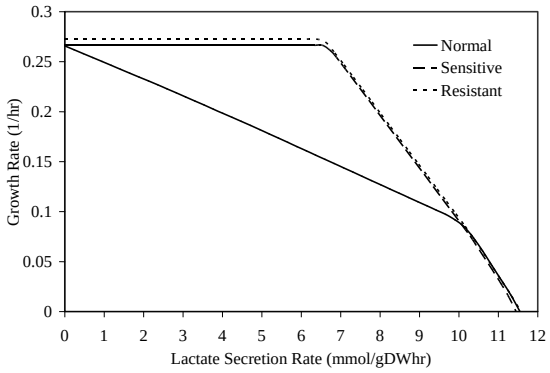

Figure 2. Growth rate sensitivity to lactate secretion rate for various cell lines

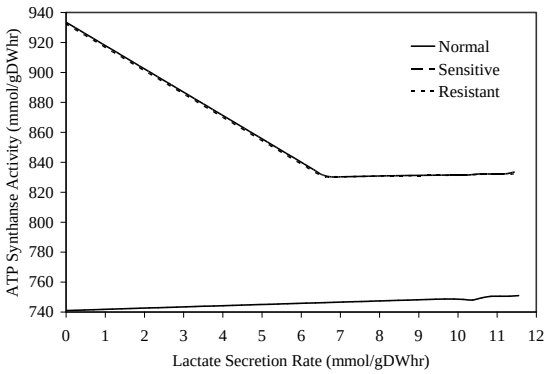

Figure 4. Change of maximum ATP synthase activity in different lactate secretion rates for various cell lines at optimal growth

In Table 2, responsible reactions for lactate secretion in cancer cells have been presented. All of them exchange malate or succinate, for phosphate or sulfate, based on antiporter system. The same gene (SLC25A10) encodes all proteins of the seven reactions. Results are identical for sensitive and resistant models.

Eight combinations of four reactions from Table 2 that their deletion causes the disability of cancer cells to secrete lactate at optimal growth have been presented in Table 3. Reaction 4 exists in all reaction sets, and therefore it is very important for lactate secretion in cancer cells based on the model predictions.

According to the model results, deletion of SLC25A10 gene reduces the growth of sensitive and resistant cells to 78 percent of wild type, while it is absent from the normal model. This gene encodes a member of a family of proteins that translocate small metabolites across the mitochondrial membrane. The encoded protein exchanges dicarboxylates, such as malate, fumarate and succinate, for phosphate, sulfate, and other small molecules and thereby providing substrates for metabolic processes including the TCA cycle and fatty acid synthesis.

Gene deletion effect

Table 4 demonstrates the results of single and double gene deletion analysis on three metabolic models using FBA approach. Computations predict that sensitive cell has one more essential gene and one less growth reducing gene compared to resistant cell. Gene FH which encodes fumarate hydratase is lethal for sensitive cells, while it is growth reducing for normal and resistant cells. Based on computational results, genes CDS1, HPRT1 and PTDSS1 encoding CDP-diacylglycerol synthase (phosphatidate cytidylyltransferase) 1, hypoxanthine phosphoribosyltransferase 1 and phosphatidylserine synthase 1, respectively, are essential only for normal cells. Deletion of most of the growth reducing genes affects less than 20 percent on growth. Growth reducing genes with GR≤0.8 are identical for

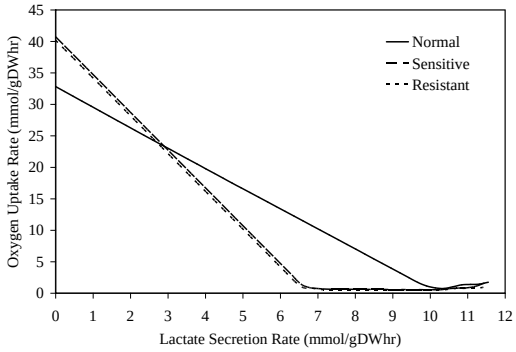

Figure 3. Change of maximum oxygen uptake rate in different lactate secretion rates for various cell lines at optimal growth

Table 2. Responsible reactions for lactate secretion in cancer cells (c, cytoplasmic; m, mitochondrial)

Reaction no.	Reaction	associated Gene
1	fumarate[c] + so4[m] <==> fumarate[m] + so4[c]	SLC25A10
2	fumarate[c] + thiosulfate [m] <==> fumarate[m] + thiosulfate [c]	SLC25A10
3	fumarate[c] + pi[m] <==> fumarate[m] + pi[c]	SLC25A10
4	malate-L[c] + so3[m] <==> malate-L[m] + so3[c]	SLC25A10
5	malate-L[c] + so4[m] <==> malate-L[m] + so4[c]	SLC25A10
6	malate-L[c] + pi[m] <==> malate-L[m] + pi[c]	SLC25A10
7	malate-L[c] + thiosulfate [m] <==> malate-L[m] + thiosulfate [c]	SLC25A10

Table 3. Eight combinations of four reactions that their deletion causes to disability of cancer cells to secrete lactate at optimal growth (reaction numbers are based on Table 2)

Group No.	Reaction no.			
1	1	2	3	4
2	1	2	4	6
3	1	3	4	7
4	1	4	6	7
5	2	3	4	5
6	2	4	5	6
7	3	4	5	7
8	4	5	6	7

Table 4. Results of single and double gene deletion analysis on three metabolic model using flux balance analysis approach

Cell line	Number of genes							
	Lethal	Sick	Sick with GR≤0.8	With interaction	With ≥5 interactions	Synthetic lethal	Snthetic sick	Synthetic sick with GR≤0.8
Resistant	74	48	9	158	57	38	738	107
Sensitive	75	47	9	150	47	22	664	94
Normal	77	64	18	178	60	36	687	183

resistant and sensitive cells although there is twice growth reducing genes with GR≤0.8 in normal cells. Therefore, there are more targeting points in normal cells metabolism to reduce the growth. This result was expected because the genes expression in normal cells has not been regulated for further growth against cancer cells.

Double gene deletion analysis demonstrates that resistant cells have the maximum synthetic lethal and sick genes even more than normal cells. The results indicate that there are more synthetic target points in resistant cells to reduce the growth. Similar to single deletion, most of the synthetic sick genes have effect on growth less than 20 percent. Interaction between genes which indicates a measure of synergism between the genes is higher in normal cells, and it is notable that interactions in resistant cells have increased in comparison with sensitive cells. Metabolism variation of resistant cancer from sensitive is more obviously in double gene deletion. Synergism between genes has increased and the metabolism is more vulnerable for growth similar to normal cells, although the difference of resistant metabolism from normal is more than sensitive metabolism. Hence, it seems that resistant cancer cells have been forced to choose a less robust metabolism with more synergisms and synthetic targeting points; however, this metabolism is resistant to cisplatin drug. These new target points introduced by the model could be used to design a new drug and break down the chemoresistance.

Among the all proposed knockouts, drug targets with minimum side-effect on normal cells that only damage the cancer cells metabolism will be appropriate. Therefore, effect of all sick, lethal, synthetic lethal and sick knockouts for the cancer cells on growth of normal cells was calculated. Furthermore, effect of gene knockout on ATP synthase activity (which is a vital biochemical reaction for energy production using oxidative phosphorylation and must be preserved in every cell) was studied (11). The results which introduce some appropriate drug targets for resistant and sensitive cancer cells have been presented in supplementary File S4.

It can be seen that all lethal genes of resistant model are also essential for normal cells growth. For lethal genes of sensitive cells, only FH (ID: 2271) is nonessential gene for the normal cells and its deletion reduces the growth to GR=0.61. Lethal genes of both cancer cells have a low impact on ATP synthase activity. All of the genes which properly reduce the cancer cells growth have side-effect on growth and oxidative phosphorylation of normal cells, and hence they are not proposed as an appropriate target. Among predicted synthetic lethal genes for cancer cells, there are two gene pairs (ALDH18A1 and SLC5A1; SLC20A1 and SLC20A2 for resistant cells, GATM and ALDH18A1; SLC20A1 and SLC20A2 for sensitive cells) which have not any impact on normal cells growth and energy production. Among synthetic sick genes, there are some appropriate double knockouts. For instance, deletion of SLC25A10 and DBT reduces the cancer cells growth to GR=0.75 and their deletion effect on normal model is negligible.

Discussion

As mentioned, Warburg proposed that aerobic glycolysis in cancer cells is the combined result of a variety of factors for instance oncogenes, tumor suppressors, a hypoxic microenvironment, mtDNA mutations, genetic background in addition to permanent impairment of mitochondrial oxidative phosphorylation. Currently, the Warburg effect is generally described by alterations in signaling pathways that govern glucose uptake and consumption, which are also involved in the regulation of mitochondrial activity rather than by mitochondrial defects; though, some aggressive cancer cells do display mitochondrial deterioration. Not only mitochondrial function in cell metabolism is restricted to ATP production for cellular demands, but also mitochondria generates reactive oxygen species (ROS), which usually participate in the regulation of multiple physiological procedures; however, it might be hurtful if produced extremely (33).

In fact, the mitochondria are potent producer of superoxide as a by-product of internal oxidative procedures such as fatty acid β-oxidation or respiratory

chain function (34). Cancer cells can change their energy supply by switching from active glycolysis to fatty acid oxidation with an associated amplify in Krebs cycle activity and oxidative phosphorylation. An induced rate of electron transport across the respiratory chain leads to a reduced steady-state level of reductive intermediates, the electron donors for superoxide generation. Apparently, the result of this is the preventing mitochondrial overload, and excessive ROS production in addition to apoptosis. It would appear that mitochondrial overload resulting in excessive ROS production and initiation of apoptosis is inhibited by high energy substrates inducing UCP's as a gearing mechanism that maintains the balance between energy productions coupled to respiration versus energy dissipation as heat (35), thereby evading the significant point of ROS excess triggering cell death. Furthermore, this finding is confirmed by the observation that methylmalonate (36) and malonate (37) as critical intermediate metabolites of fatty acid metabolism inhibit dicarboxylate transporter and complex II SDH respiratory chain function (38), yet increase ROS leading to apoptosis. Additionally, it has been investigated that fatty acids by themselves can operate as mitochondrial uncouplers and inhibitors of pyruvate oxidation (39).

Consequently, these sides of fatty acid metabolism must be overcome if cancer cells are to survive, and this is one function of UCP-2. In addition, it was suggested that fatty acid oxidation in cancer cells was linked to chemoresistance and mitochondrial uncoupling by UCP that Warburg's observations cleared the preferential oxidation of fatty acids by cancer cell mitochondria. Therefore, targeting fatty acid oxidation or anaplerotic pathways that support fatty acid oxidation could offer a new efficient tumor therapy (40).

Based on pointed investigations, inhabitation of dicarboxylate transporter, which encoded by SLC25A10 may play critical role in preventing the flow of citrate or succinate and then inducing of the oxidative stress, ROS production excessively and inducing apoptotic cascade in cancer cells. The mentioned findings can support the significance of dicarboxylate transporter as the product of SLC25A10 gene in increasing maintenance and growth capacities of cancer cells via involving Warburg phenomenon.

Hence, SLC25A10 gene knockout helps to eliminate one of the important ability of cancer cells for high proliferation. It may solve how diverse cancers adapt the procedures to complete their metabolic requirements. In addition to elimination of Warburg effect, targeting the SLC25A10 gene is valuable because this gene is unexpressed in normal cells, and hence its knockout does not have side-effect for them.

According to the results, metabolic models are capable to truly show cancer cells ability to secrete lactate, while they are growing fast and the models introduced a target gene to omit this phenotype. Therefore, the metabolic models could be used to propose the new drug targets, which prevent the rapid growth of cancer cells. The metabolic models were used to propose single and double gene knockouts that result in death of cancer cells. The effect of these gene knockouts on growth and energy production of normal cells was estimated using the normal model.

Conclusion

In this research, transcription data was used to determine absent and present genes in cancer and normal cell lines. Then, the generic human metabolic model was reduced to the resistant and sensitive cancer and normal ovarian cells specific model by removing the absent genes using the GIMME algorithm. Cell line specific metabolic models were studied to determine the effect of various gene expressions of cells on the metabolism. Algorithmic reconstructed metabolic models present various metabolism usages, especially for normal and cancer cells. Reactions from various pathways were activated or deactivated to form the cancerous metabolism.

The models were used to study the aerobic glycolysis and Warburg effect in cancer cells as a known phenotype. Based on simulation of cancer and normal cells growth, this hypothesis can be considered that secretion of lactate may be due to the oxygen limitation in tissue for proliferation with maximum rate. In fact, cancer cells against normal cells are able to reduce oxygen demand with secretion of lactate, while this secretion do not affect on proliferation rate. In addition, our results identify that cancer cells reduce activity of ATP synthase enzyme with lactate secretion, while normal cells are not able to do it. Comparison of metabolisms identified that SLC25A10 gene is responsible for this phenotype of cancer cells. The experimental facts that inhibiting dicarboxylate transporter (as the SLC25A10 product) can exhibit ROS production, and ROS are critically involved in the regulation of cell death pathways, apoptosis as well as necrosis can validate the current *in silico* model in addition to importance of targeting of mitochondrial alterations in tumor cells for the development of novel efficient chemotherapy.

After studying the Warburg effect and clarifying the model ability to illustrate cancerous and normal cells metabolism difference, the model was used to study the effect of single and double gene deletion on growth. New single and double drug targets were proposed, which could reduce the cancer cells growth. Furthermore, computational data indicate that double gene knockout proposes more appropriate targets with minimum side-effect on normal cells growth and energy production. The

double knockout analyses also indicate that cisplatin cause a more vulnerable metabolism for resistant cells compared with sensitive cells although it does not cause apoptosis.

Acknowledgment

The authors wish to thank Pasteur Institute of Iran for supporting the first author.

References

1. Li M, Balch C, Montgomery J, Jeong M, Chung J, Yan P, *et al*. Integrated analysis of DNA methylation and gene expression reveals specific signaling pathways associated with platinum resistance in ovarian cancer. BMC Medical Genomics 2009; 2:34.
2. McGuire WP, Hoskins WJ, Brady MF, Kucera PR, Partridge EE, Look KY, *et al*. Cyclophosphamide and cisplatin compared with paclitaxel and cisplatin in patients with stage iii and stage iv ovarian cancer. N Engl J Med 1996; 334:1-6.
3. Agarwal R, Kaye SB. Ovarian cancer: strategies for overcoming resistance to chemotherapy. Nat Rev Cancer 2003; 3:502-516.
4. Stewart DJ. Mechanisms of resistance to cisplatin and carboplatin. Crit Rev Oncol Hematol 2007; 63:12-31.
5. Bordbar A, Palsson BO. Using the reconstructed genome-scale human metabolic network to study physiology and pathology. J Intern Med 2012; 271:131-141.
6. Shalamzari SA, Agha-Alinejad H, Alizadeh S, Shahbazi S, Khatib ZK, Kazemi A, *et al*. The effect of exercise training on the level of tissue IL-6 and vascular endothelial growth factor in breast cancer bearing mice. Iran J Basic Med Sci 2014; 17:231-258.
7. Jones NP, Schulze A. Targeting cancer metabolism–aiming at a tumour's sweet-spot. Drug Discov Today 2012; 17:232-241.
8. Thiele I, Palsson BO. A protocol for generating a high-quality genome-scale metabolic reconstruction. Nat Protoc 2010; 5:93-121.
9. Duarte NC, Becker SA, Jamshidi N, Thiele I, Mo ML, Vo TD, *et al*. Global reconstruction of the human metabolic network based on genomic and bibliomic data. Proc Natl Acad Sci 2007; 104:1777-1782.
10. Thiele I, Swainston N, Fleming RMT, Hoppe A, Sahoo S, Aurich MK, *et al*. A community-driven global reconstruction of human metabolism. Nat Biotechnol 2013; 31:419-425.
11. Folger O, Jerby L, Frezza C, Gottlieb E, Ruppin E, Shlomi T. Predicting selective drug targets in cancer through metabolic networks. Mol Syst Biol 2011; 7:501.
12. DeBerardinis RJ, Lum JJ, Hatzivassiliou G, Thompson CB. The biology of cancer: metabolic reprogramming fuels cell growth and proliferation. Cell Metab 2008; 7:11-20.
13. Tennant DA, Durán RV, Boulahbel H, Gottlieb E. Metabolic transformation in cancer. Carcinogenesis 2009; 30:1269-1280.
14. Price ND, Reed JL, Palsson BO. Genome-scale models of microbial cells: evaluating the consequences of constraints. Nat Rev Microbiol 2004; 2:886-897.
15. Motamedian E, Naeimpoor F. Prediction of proton exchange and bacterial growth on various substrates using constraint-based modeling approach. Biotechnol Bioproc E 2011; 16:875-84.
16. Shlomi T, Benyamini T, Gottlieb E, Sharan R, Ruppin E. Genome-scale metabolic modeling elucidates the role of proliferative adaptation in causing the Warburg effect. PLoS Comput Biol 2011; 7:e1002018.
17. Blazier AS, Papin JA. Integration of expression data in genome-scale metabolic network reconstructions. Front Physiol 2012; 3:299.
18. Becker SA, Palsson BO. Context-specific metabolic networks are consistent with experiments. PLoS Comput Biol 2008; 4:e1000082.
19. Colijn C, Brandes A, Zucker J, Lun DS, Weiner B, Farhat MR, *et al*. Interpreting expression data with metabolic flux models: predicting *Mycobacterium tuberculosis* mycolic acid production. PLoS Comput Biol 2009; 5:e1000489.
20. Shlomi T, Cabili MN, Herrgard MJ, Palsson BO, Ruppin E. Network-based prediction of human tissue-specific metabolism. Nature Biotech 2008; 26:1003-1010.
21. Moxley JF, Jewett MC, Antoniewicz MR, Villas-Boas SG, Alper H, Wheeler RT, *et al*. Linking high-resolution metabolic flux phenotypes and transcriptional regulation in yeast modulated by the global regulator Gcn4p. Proc Natl Acad Sci USA 2009; 106:6477-6482.
22. Jensen PA, Papin JA. Functional integration of a metabolic network model and expression data without arbitrary thresholding. Bioinformatics 2011; 27:541-547.
23. Kim J, Reed JL. RELATCH: relative optimality in metabolic networks explains robust metabolic and regulatory responses to perturbations. Genome Biol 2012; 13:R78.
24. Agren R, Bordel S, Mardinoglu A, Pornputtapong N, Nookaew I, Nielsen J. Reconstruction of genome-scale active metabolic networks for 69 human cell types and 16 cancer types using INIT. PLoS Comput Biol 2012; 8:e1002518.
25. Wang Y, Eddy JA, Price ND. Reconstruction of genome-scale metabolic models for 126 human tissues using mCADRE. BMC Syst Biol 2012; 6:153.
26. Li L, Zhou X, Ching WK, Wang P. Predicting enzyme targets for cancer drugs by profiling human metabolic reactions in NCI-60 cell lines. BMC Bioinformatics 2010; 11:501.
27. Jerby L, Wolf L, Denkert C, Stein GY, Hilvo M, Oresic M, *et al*. Metabolic associations of reduced proliferation and oxidative stress in advanced breast cancer. Cancer Res 2012; 72:5712-5720.
28. Becker SA, Palsson BO. Context-specific metabolic networks are consistent with experiments. PLoS Comput Biol 2008; 4:e1000082.
29. Pepper S, Saunders E, Edwards L, Wilson C, Miller C. The utility of MAS5 expression summary and detection call algorithms. BMC Bioinformatics 2007; 8:273.
30. Stany MP, Vathipadiekal V, Ozbun L, Stone RL, Mok SC, Xue H, *et al*. Identification of novel therapeutic targets in microdissected clear cell ovarian cancers. PLoS One 2011; 6:e21121.

31. Schellenberger J, Que R, Fleming RMT, Thiele I, Orth JD, Feist AM, *et al*. Quantitative prediction of cellular metabolism with constraint-based models: the COBRA Toolbox v2.0. Nat Protoc 2011; 6:1290-1307.
32. Gogvadze V, Zhivotovsky B, Orrenius S. The Warburg effect and mitochondrial stability in cancer cells. Mol Aspects Med 2010; 31:60-74.
33. Ralph SJ, Rodríguez-Enríquez S, Neuzil J, Moreno-Sánchez R. Bioenergetic pathways in tumor mitochondria as targets for cancer therapy and the importance of the ROS-induced apoptotic trigger. Mol Aspects Med 2010; 31:29-59.
34. Echtay KS, Roussel D, St-Pierre J, Jekabsons MB, Cadenas S, Stuart JA, *et al*. Superoxide activates mitochondrial uncoupling proteins. Nature 2002; 415:96-99.
35. Toyoshima S, Watanabe F, Saido H, Miyatake K, Nakano Y. Methylmalonic Acid Inhibits Respiration in Rat Liver Mitochondria. J Nutr 1995; 125:2846-2850.
36. Fernandez-Gomez FJ, Galindo MF, Gómez-Lázaro M, Yuste VJ, Comella JX, Aguirre N, *et al*. Malonate induces cell death via mitochondrial potential collapse and delayed swelling through an ROS-dependent pathway. Br J Pharmacol 2005; 144:528-537.
37. Mirandola SR, Melo DR, Schuck PF, Ferreira GC, Wajner M, Castilho RF. Methylmalonate inhibits succinate-supported oxygen consumption by interfering with mitochondrial succinate uptake. J Inherit Metab Dis 2008; 31:44-54.
38. Koga Y, Yoshino M, Yamashita F. Effects of short and medium chain length fatty acids on pyruvate oxidation by cultured human fibroblasts and rat liver mitochondria. J Inherit Metab Dis 1984; 7:141-142.
39. Samudio I, Fiegl M, Andreeff M. Mitochondrial uncoupling and the Warburg effect: molecular basis for the reprogramming of cancer cell metabolism. Cancer Res 2009; 69:2163-2166.